

Supporting Information

Tetrahedral node diamondyne frameworks for CO₂ adsorption and separation

Ling Huang, Xiaofei Zeng and Dapeng Cao*

Division of Molecular and Materials Simulation, State Key Lab of Organic-Inorganic Composites, Beijing University of Chemical Technology, Beijing 100029, China.

Email: caodp@mail.buct.edu.cn

1. Computational Details

The geometrical optimizations were performed *via* Vienna *ab-initio* simulation package (VASP),¹ where the projected augmented wave generalized gradient approximation (PAW-LDA) method was adopted. All the structures were optimized aiming at the global energy minimum, and fully relaxed until the residual force convergence value on each atom is less than 0.01eV/Å. The Brillouin zone was sampled with a set of K-point grid (5×5×5) according to the Monkhorst-Pack scheme, which is large enough in our calculations. As a result, both TND-1 and TND-2 belong to the cubic space group P1 with unit cell parameters (a=b=c) of 21.9871 and 15.6602 Å, respectively. In addition, the pore size of tetrahedron is ~4 Å, while for the outer maintained diamond-like cavity, they are 17 Å and 11 Å in TND-1 and TND-2, respectively. In addition, the angle of C-C≡C is about 158°, which is comparable with what has been reported by Diederich (161°),² and the density of TND-1 and TND-2 are respectively 0.30 and 0.66 g/cm³. Moreover, the calculated BET surface area for TND-1 and TND-2 are 6250 and 2990 m²/g, respectively. The formation energy of TND-1 and TND-2 are 1.164 and 1.091 eV/atom, indicating the thermodynamics stability for both two configurations.

Furthermore, both adsorption and separation behaviors at ambient condition were explored by Grand Canonical Monte Carlo (GCMC) simulation in MUSIC program package.³ During the GCMC simulation, periodic boundary conditions were imposed in

all three directions and the LJ potentials were cut off at the position of the half of the minimal box size. For each pressure point, 3×10^7 configurations were generated, where the first 1.5×10^7 configurations were discarded to guarantee equilibration and the second 1.5×10^7 configurations were divided into 10 blocks to calculate the ensemble average. The uncertainties of the final results, including the ensemble averages of the number of adsorbate molecules in the simulation cell and the total potential energy, were estimated to be within $\pm 2\%$.

Table S1. LJ parameters (ϵ/k_B [K], σ [Å]) for CO₂, CH₄, N₂, H₂ and adsorbents (TND-1 and TND-2), respectively.

	C-CO ₂	O-CO ₂	CH ₄	N ₂	H ₂	C-TND-1	C-TND-2
ϵ/k_B [K]	27.0	79.0	148.0	94.95	36.7	47.9	
σ [Å]	2.80	3.05	3.73	3.549	2.958	3.47	
q [e]	0.70	-0.35	0	0	0	0	

Table S1 gives the LJ parameters for adsorbates and adsorbent used in GCMC simulations. LJ parameters for framework atom (all carbon) was assigned based on the DREIDING force field⁴ and CO₂ was modeled using the TraPPE force field of Potoff and Siepmann,⁵ where a 3-site CO₂ model with LJ parameters and partial charges imposed to best reproduce experimental CO₂ vapor-liquid equilibrium data. Here in the simulation of CO₂ adsorption, we only considered the electrostatic interaction of inter- & intra- CO₂ molecules, and ignored the atomic charges of the TND-1 and TND-2, for the fact that there is no metal atom in them. CH₄⁶ and H₂⁷ were represented by spherical united-atom model, while for the 1-site model of N₂,⁸ we adopted the LJ parameters from Kaneko and Seaton et al. The set of parameters has already been successfully used in our recent work by Yang et al., and the accuracy for calculations was guaranteed.⁹ In addition, the Lorentz-Berthelot combining rules were used to calculate the cross-interaction parameters, and interactions were cut off at a distance of 14.0 Å.

In this work, to obtain the pore volume V_{pore} , we used the method of Myers *et al.* from the idea gas law (Eq. S1)¹⁰

$$V_{pore} = \frac{RN_m T}{Pm_m}$$

where R is the gas constant, T is the temperature, P is the pressure, and N_m is the number of adsorbed probe molecules per molar mass m_m of the adsorbents.

In addition, we calculated the isosteric heat, Q_{st} , which reflects the released heat for each molecule added to the adsorbed phase, by the following equation (Eq. S2)¹¹

$$Q_{st} = \frac{\langle U \rangle \langle N \rangle - \langle UN \rangle}{\langle N^2 \rangle - \langle N \rangle \langle N \rangle} + k_B T$$

where $\langle \dots \rangle$ denotes the ensemble average, N is the number of particles, and U is the configuration energy of system.

The adsorption selectivity S is a good indicator to evaluate the separation property of nanoporous materials for equilibrium separation process. Here, the adsorption selectivity (Eq. S3) of component i over j in a binary mixture is defined as

$$S = \left(\frac{x_i}{x_j} \right)_{pore} / \left(\frac{y_i}{y_j} \right)_{bulk}$$

where x and y represent the molar fractions of components in the adsorbed and bulk phases, respectively.

2. Snapshots

To intuitively illustrate the selectivity trend of CO₂/H₂ in TND-2 frameworks, Figure S1 shows snapshots of binary mixture (CO₂/H₂) adsorbed in TND-2. CO₂ and H₂ were marked in red and green, respectively. It can be seen that, at low pressures, the adsorbed adsorbates mainly accumulated on the surface of substrates. Moreover, there is no molecule entering the tetrahedron, due to the insufficient pore size (~4 Å) with respect to the molecular dynamical diameter of CO₂ (3.3 Å), CH₄ (3.76 Å), N₂ (3.64 Å), and H₂ (2.89 Å).¹² In addition, at low pressure, the uptake of both CO₂ and H₂ are increasing with pressure rising (see Figure S1a, b and c); while pressure is high, the situation is changing, namely the speed for the increase of H₂ exceeds that of CO₂ (see Figure S1d, e and f) because the adsorption of CO₂ tends to saturation amount and remains unchanged while H₂ with the smaller molecular diameter can still enter the pore, hence resulting in the phenomenon that the selectivity of CO₂/H₂ shall be increasing at low pressure and

decreasing when pressure continues to rise. The snapshots provide a good microscopic explanation for the adsorptive separation of CO₂ over H₂ in TND-2 shown in Figure 3 (corresponding to the state point of A, B, C, D, E, and F).

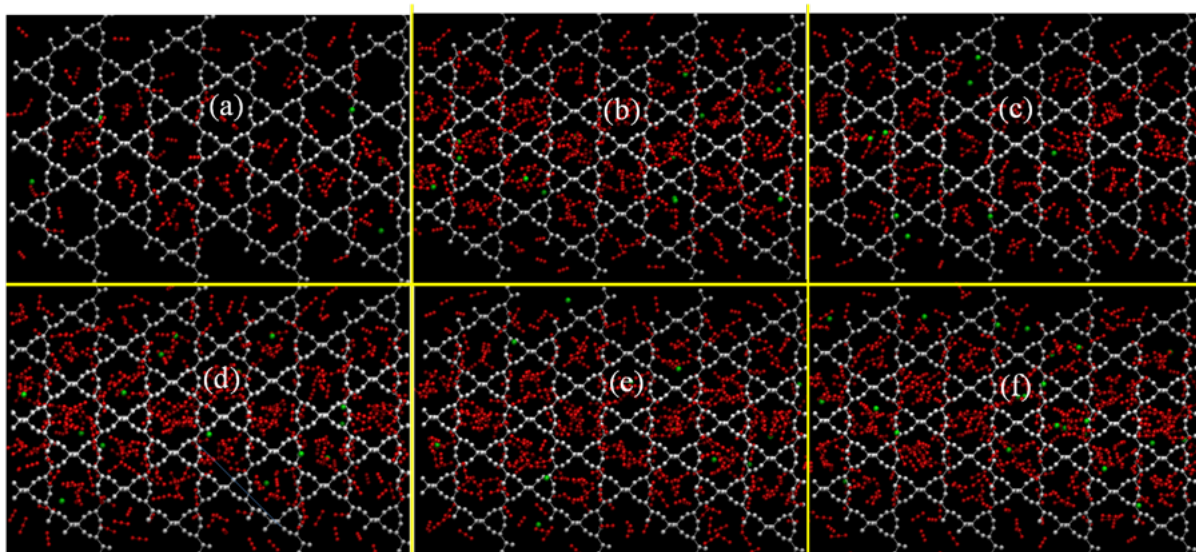


Figure S1. The snapshots for selectivity of CO₂/H₂ in TND-2, the simulation box for TND-2 in GCMC calculations is the 4×2×2 unit cell. (a)~(f) denotes the configuration at pressure of 5, 15, 30, 50, 80, and 100 bar, respectively.

References

- (1) G. Kresse; J. Furthmüller *Phys. Rev. B* **1996**, *54*, 11169.
- (2) F. Diederich *Nature* **1994**, *369*, 199.
- (3) A. Gupta; S. Chempath; M. J. Sanborn; L. A. Clark; R. Q. Snurr *Mol. Simul.* **2003**, *29*, 29.
- (4) S. L. Mayo; B. D. Olafson; W. A. Goddard *J Phys. Chem.* **1990**, *94*, 8897.
- (5) J. J. Potoff; J. I. Siepmann *Aiche J* **2001**, *47*, 1676.
- (6) E. D. Bloch; W. L. Queen; R. Krishna; J. M. Zadrozny; C. M. Brown; J. R. Long *Science* **2012**, *335*, 1606.
- (7) D. Levesque; A. Gicquel; F. L. Darkrim; S. B. Kayiran *J Phys.-Condens. Mat.* **2002**, *14*, 9285.
- (8) T. Ohkubo; J. Miyawaki; K. Kaneko; R. Ryoo; N. A. Seaton *J Phys.Chem. B* **2002**, *106*, 6523.
- (9) Z. L. Yang; X. Peng; D. P. Cao *J Phys. Chem. C* **2013**, *117*, 8353.
- (10) (a)A. L. Myers; P. A. Monson *Langmuir* **2002**, *18*, 10261; (b)O. Talu; A. L. Myers *Aiche J* **2001**, *47*, 1160.
- (11) J. H. Lan; D. P. Cao; W. C. Wang *Langmuir* **2010**, *26*, 220.
- (12) H. Y. Zhao; Z. Jin; H. M. Su; J. L. Zhang; X. D. Yao; H. J. Zhao; G. S. Zhu *Chem. Commun.* **2013**, *49*, 2780.

TND-1 CIF Data

```
data_T-opt
_audit_creation_date      2013-07-17
_audit_creation_method    'Materials Studio'
_symmetry_space_group_name_H-M  'P1'
_symmetry_Int_Tables_number  1
_symmetry_cell_setting    triclinic
loop_
_symmetry_equiv_pos_as_xyz
  x,y,z
_cell_length_a            21.9871
_cell_length_b            21.9871
_cell_length_c            21.9871
_cell_angle_alpha         90.0000
_cell_angle_beta          90.0000
_cell_angle_gamma         90.0000
loop_
_atom_site_label
_atom_site_type_symbol
_atom_site_fract_x
_atom_site_fract_y
_atom_site_fract_z
_atom_site_U_iso_or_equiv
_atom_site_adp_type
_atom_site_occupancy
C1      C      0.18117  0.18118  0.18117  0.00000  Uiso  1.00
C2      C      0.18118  0.31882  0.31882  0.00000  Uiso  1.00
C3      C      0.31893  0.31893  0.18137  0.00000  Uiso  1.00
C4      C      0.31882  0.18118  0.31882  0.00000  Uiso  1.00
C5      C      0.18117  0.68117  0.68117  0.00000  Uiso  1.00
C6      C      0.68117  0.68117  0.18117  0.00000  Uiso  1.00
C7      C      0.68117  0.18117  0.68117  0.00000  Uiso  1.00
C8      C      0.81883  0.18117  0.81883  0.00000  Uiso  1.00
C9      C      0.18117  0.81883  0.81883  0.00000  Uiso  1.00
C10     C      0.81883  0.81883  0.18117  0.00000  Uiso  1.00
C11     C      0.93118  0.56882  0.43118  0.00000  Uiso  1.00
C12     C      0.81882  0.68118  0.31882  0.00000  Uiso  1.00
C13     C      0.81882  0.31882  0.68118  0.00000  Uiso  1.00
C14     C      0.93118  0.43118  0.56882  0.00000  Uiso  1.00
C15     C      0.31882  0.68118  0.81882  0.00000  Uiso  1.00
C16     C      0.43118  0.56882  0.93118  0.00000  Uiso  1.00
C17     C      0.56882  0.43118  0.93118  0.00000  Uiso  1.00
```

C18	C	0.68118	0.31882	0.81882	0.00000	Uiso	1.00
C19	C	0.68118	0.81882	0.31882	0.00000	Uiso	1.00
C20	C	0.56882	0.93118	0.43118	0.00000	Uiso	1.00
C21	C	0.31882	0.81882	0.68118	0.00000	Uiso	1.00
C22	C	0.43118	0.93118	0.56882	0.00000	Uiso	1.00
C23	C	0.39126	0.89125	0.60877	0.00000	Uiso	1.00
C24	C	0.35875	0.85874	0.64124	0.00000	Uiso	1.00
C25	C	0.14123	0.64126	0.64125	0.00000	Uiso	1.00
C26	C	0.10875	0.60876	0.60874	0.00000	Uiso	1.00
C27	C	0.14123	0.85874	0.85875	0.00000	Uiso	1.00
C28	C	0.10874	0.89125	0.89125	0.00000	Uiso	1.00
C29	C	0.35874	0.64124	0.85874	0.00000	Uiso	1.00
C30	C	0.39124	0.60875	0.89125	0.00000	Uiso	1.00
C31	C	0.64123	0.85873	0.35874	0.00000	Uiso	1.00
C32	C	0.60873	0.89123	0.39124	0.00000	Uiso	1.00
C33	C	0.14124	0.35872	0.35876	0.00000	Uiso	1.00
C34	C	0.10873	0.39123	0.39125	0.00000	Uiso	1.00
C35	C	0.64125	0.35874	0.85876	0.00000	Uiso	1.00
C36	C	0.60874	0.39124	0.89124	0.00000	Uiso	1.00
C37	C	0.89124	0.89126	0.10874	0.00000	Uiso	1.00
C38	C	0.85875	0.85874	0.14123	0.00000	Uiso	1.00
C39	C	0.10876	0.10876	0.10873	0.00000	Uiso	1.00
C40	C	0.14125	0.14126	0.14124	0.00000	Uiso	1.00
C41	C	0.89124	0.10873	0.89124	0.00000	Uiso	1.00
C42	C	0.85874	0.14122	0.85874	0.00000	Uiso	1.00
C43	C	0.60876	0.10875	0.60873	0.00000	Uiso	1.00
C44	C	0.64127	0.14124	0.64124	0.00000	Uiso	1.00
C45	C	0.35874	0.14126	0.35876	0.00000	Uiso	1.00
C46	C	0.39125	0.10875	0.39124	0.00000	Uiso	1.00
C47	C	0.35882	0.35882	0.14138	0.00000	Uiso	1.00
C48	C	0.39128	0.39128	0.10881	0.00000	Uiso	1.00
C49	C	0.85875	0.64126	0.35875	0.00000	Uiso	1.00
C50	C	0.89125	0.60876	0.39125	0.00000	Uiso	1.00
C51	C	0.60875	0.60876	0.10874	0.00000	Uiso	1.00
C52	C	0.64123	0.64125	0.14125	0.00000	Uiso	1.00
C53	C	0.89124	0.39124	0.60874	0.00000	Uiso	1.00
C54	C	0.85874	0.35875	0.64125	0.00000	Uiso	1.00
C55	C	0.77094	0.34807	0.72906	0.00000	Uiso	1.00
C56	C	0.72906	0.34806	0.77094	0.00000	Uiso	1.00
C57	C	0.77094	0.27094	0.65194	0.00000	Uiso	1.00
C58	C	0.72906	0.22906	0.65194	0.00000	Uiso	1.00
C59	C	0.65192	0.22906	0.72906	0.00000	Uiso	1.00
C60	C	0.65192	0.27094	0.77094	0.00000	Uiso	1.00
C61	C	0.77094	0.15194	0.77094	0.00000	Uiso	1.00
C62	C	0.72906	0.15194	0.72907	0.00000	Uiso	1.00

C63	C	0.72906	0.27094	0.84806	0.00000	Uiso	1.00
C64	C	0.77094	0.22906	0.84806	0.00000	Uiso	1.00
C65	C	0.84807	0.27094	0.72907	0.00000	Uiso	1.00
C66	C	0.84807	0.22905	0.77095	0.00000	Uiso	1.00
C67	C	0.27094	0.84806	0.72907	0.00000	Uiso	1.00
C68	C	0.22906	0.84807	0.77095	0.00000	Uiso	1.00
C69	C	0.22905	0.77095	0.84807	0.00000	Uiso	1.00
C70	C	0.27094	0.72906	0.84806	0.00000	Uiso	1.00
C71	C	0.34806	0.72906	0.77094	0.00000	Uiso	1.00
C72	C	0.34806	0.77094	0.72906	0.00000	Uiso	1.00
C73	C	0.15193	0.77094	0.77094	0.00000	Uiso	1.00
C74	C	0.15193	0.72906	0.72906	0.00000	Uiso	1.00
C75	C	0.27093	0.65194	0.77094	0.00000	Uiso	1.00
C76	C	0.22905	0.65193	0.72906	0.00000	Uiso	1.00
C77	C	0.27094	0.77094	0.65193	0.00000	Uiso	1.00
C78	C	0.22906	0.72906	0.65193	0.00000	Uiso	1.00
C79	C	0.22908	0.34811	0.27102	0.00000	Uiso	1.00
C80	C	0.27102	0.34816	0.22920	0.00000	Uiso	1.00
C81	C	0.34811	0.22909	0.27102	0.00000	Uiso	1.00
C82	C	0.34815	0.27101	0.22920	0.00000	Uiso	1.00
C83	C	0.22904	0.27092	0.34806	0.00000	Uiso	1.00
C84	C	0.27092	0.22905	0.34806	0.00000	Uiso	1.00
C85	C	0.22911	0.22912	0.15203	0.00000	Uiso	1.00
C86	C	0.27101	0.27102	0.15210	0.00000	Uiso	1.00
C87	C	0.22905	0.15193	0.22906	0.00000	Uiso	1.00
C88	C	0.27094	0.15193	0.27093	0.00000	Uiso	1.00
C89	C	0.15192	0.22905	0.22905	0.00000	Uiso	1.00
C90	C	0.15193	0.27094	0.27092	0.00000	Uiso	1.00
C91	C	0.72905	0.65193	0.22906	0.00000	Uiso	1.00
C92	C	0.77094	0.65194	0.27094	0.00000	Uiso	1.00
C93	C	0.77093	0.72906	0.34806	0.00000	Uiso	1.00
C94	C	0.72905	0.77094	0.34807	0.00000	Uiso	1.00
C95	C	0.65194	0.72906	0.22906	0.00000	Uiso	1.00
C96	C	0.65194	0.77094	0.27093	0.00000	Uiso	1.00
C97	C	0.72906	0.72906	0.15193	0.00000	Uiso	1.00
C98	C	0.77094	0.77094	0.15193	0.00000	Uiso	1.00
C99	C	0.84806	0.72906	0.27093	0.00000	Uiso	1.00
C100	C	0.84807	0.77094	0.22906	0.00000	Uiso	1.00
C101	C	0.72906	0.84807	0.27094	0.00000	Uiso	1.00
C102	C	0.77095	0.84807	0.22906	0.00000	Uiso	1.00
C103	C	0.47906	0.52094	0.90194	0.00000	Uiso	1.00
C104	C	0.52094	0.47906	0.90194	0.00000	Uiso	1.00
C105	C	0.90194	0.47905	0.52093	0.00000	Uiso	1.00
C106	C	0.90194	0.52094	0.47906	0.00000	Uiso	1.00
C107	C	0.52095	0.52094	0.09806	0.00000	Uiso	1.00

C108	C	0.47906	0.90193	0.52094	0.00000	Uiso	1.00
C109	C	0.52094	0.90194	0.47907	0.00000	Uiso	1.00
C110	C	0.43118	0.43118	1.06882	0.00000	Uiso	1.00
C111	C	0.56882	0.56882	1.06882	0.00000	Uiso	1.00
C112	C	0.93118	0.93118	1.06882	0.00000	Uiso	1.00
C113	C	0.47907	0.47906	1.09805	0.00000	Uiso	1.00
C114	C	0.40193	0.52093	0.97906	0.00000	Uiso	1.00
C115	C	0.40193	0.47906	1.02094	0.00000	Uiso	1.00
C116	C	0.47905	0.59807	0.97906	0.00000	Uiso	1.00
C117	C	0.52093	0.59807	1.02094	0.00000	Uiso	1.00
C118	C	0.59807	0.47906	0.97906	0.00000	Uiso	1.00
C119	C	0.59807	0.52094	1.02094	0.00000	Uiso	1.00
C120	C	0.52093	0.40194	0.97906	0.00000	Uiso	1.00
C121	C	0.47905	0.40192	1.02095	0.00000	Uiso	1.00
C122	C	0.43118	1.06882	0.43118	0.00000	Uiso	1.00
C123	C	0.56882	1.06882	0.56882	0.00000	Uiso	1.00
C124	C	0.93118	1.06882	0.93118	0.00000	Uiso	1.00
C125	C	0.52094	1.09806	0.52094	0.00000	Uiso	1.00
C126	C	0.47905	1.09807	0.47906	0.00000	Uiso	1.00
C127	C	0.47906	1.02094	0.40194	0.00000	Uiso	1.00
C128	C	0.52094	0.97906	0.40194	0.00000	Uiso	1.00
C129	C	0.52095	1.02094	0.59807	0.00000	Uiso	1.00
C130	C	0.47906	0.97906	0.59806	0.00000	Uiso	1.00
C131	C	0.59806	1.02094	0.52094	0.00000	Uiso	1.00
C132	C	0.59807	0.97906	0.47906	0.00000	Uiso	1.00
C133	C	0.40193	1.02094	0.47906	0.00000	Uiso	1.00
C134	C	0.40194	0.97906	0.52095	0.00000	Uiso	1.00
C135	C	1.06882	0.43118	0.43118	0.00000	Uiso	1.00
C136	C	1.06882	0.56882	0.56882	0.00000	Uiso	1.00
C137	C	1.06882	0.93118	0.93118	0.00000	Uiso	1.00
C138	C	1.09806	0.52094	0.52094	0.00000	Uiso	1.00
C139	C	1.09807	0.47906	0.47906	0.00000	Uiso	1.00
C140	C	1.06882	1.06882	1.06882	0.00000	Uiso	1.00
C141	C	1.02094	0.97906	0.90194	0.00000	Uiso	1.00
C142	C	0.97906	1.02094	0.90193	0.00000	Uiso	1.00
C143	C	1.02093	1.09807	1.02095	0.00000	Uiso	1.00
C144	C	0.97906	1.09807	0.97906	0.00000	Uiso	1.00
C145	C	1.02094	0.52094	0.59807	0.00000	Uiso	1.00
C146	C	0.97906	0.47907	0.59807	0.00000	Uiso	1.00
C147	C	1.02093	0.59806	0.52094	0.00000	Uiso	1.00
C148	C	0.97905	0.59807	0.47906	0.00000	Uiso	1.00
C149	C	1.02094	0.40194	0.47906	0.00000	Uiso	1.00
C150	C	0.97906	0.40193	0.52094	0.00000	Uiso	1.00
C151	C	0.97906	0.52094	0.40193	0.00000	Uiso	1.00
C152	C	1.02095	0.47906	0.40193	0.00000	Uiso	1.00

C153	C	1.02094	1.02094	1.09807	0.00000	Uiso	1.00
C154	C	0.97906	0.97906	1.09807	0.00000	Uiso	1.00
C155	C	1.02093	0.90194	0.97906	0.00000	Uiso	1.00
C156	C	0.97906	0.90193	1.02094	0.00000	Uiso	1.00
C157	C	0.90194	1.02094	0.97906	0.00000	Uiso	1.00
C158	C	0.90194	0.97906	1.02094	0.00000	Uiso	1.00
C159	C	1.09806	1.02094	1.02094	0.00000	Uiso	1.00
C160	C	1.09807	0.97906	0.97906	0.00000	Uiso	1.00

loop_

_geom_bond_atom_site_label_1

_geom_bond_atom_site_label_2

_geom_bond_distance

_geom_bond_site_symmetry_2

_ccdc_geom_bond_type

C1	C89	1.622	.	S
C1	C85	1.623	.	S
C1	C87	1.622	.	S
C1	C40	1.520	.	S
C2	C83	1.622	.	S
C2	C79	1.621	.	S
C2	C90	1.622	.	S
C2	C33	1.521	.	S
C3	C82	1.621	.	S
C3	C80	1.621	.	S
C3	C86	1.623	.	S
C3	C47	1.520	.	S
C4	C81	1.621	.	S
C4	C84	1.622	.	S
C4	C88	1.622	.	S
C4	C45	1.521	.	S
C5	C76	1.622	.	S
C5	C74	1.622	.	S
C5	C78	1.622	.	S
C5	C25	1.520	.	S
C6	C95	1.622	.	S
C6	C97	1.622	.	S
C6	C91	1.622	.	S
C6	C52	1.520	.	S
C7	C58	1.622	.	S
C7	C59	1.622	.	S
C7	C44	1.520	.	S
C7	C62	1.622	.	S
C8	C61	1.622	.	S
C8	C66	1.622	.	S
C8	C64	1.622	.	S

C8	C42	1.520	.	S
C9	C69	1.622	.	S
C9	C73	1.622	.	S
C9	C68	1.622	.	S
C9	C27	1.520	.	S
C10	C102	1.622	.	S
C10	C98	1.622	.	S
C10	C100	1.622	.	S
C10	C38	1.520	.	S
C11	C106	1.622	.	S
C11	C148	1.622	.	S
C11	C151	1.622	.	S
C11	C50	1.521	.	S
C12	C99	1.622	.	S
C12	C92	1.622	.	S
C12	C93	1.622	.	S
C12	C49	1.521	.	S
C13	C65	1.622	.	S
C13	C57	1.622	.	S
C13	C55	1.622	.	S
C13	C54	1.521	.	S
C14	C105	1.622	.	S
C14	C146	1.622	.	S
C14	C150	1.622	.	S
C14	C53	1.521	.	S
C15	C70	1.622	.	S
C15	C75	1.622	.	S
C15	C71	1.622	.	S
C15	C29	1.521	.	S
C16	C103	1.622	.	S
C16	C114	1.622	.	S
C16	C116	1.622	.	S
C16	C30	1.521	.	S
C17	C104	1.622	.	S
C17	C118	1.622	.	S
C17	C120	1.622	.	S
C17	C36	1.521	.	S
C18	C63	1.622	.	S
C18	C60	1.622	.	S
C18	C56	1.622	.	S
C18	C35	1.521	.	S
C19	C101	1.622	.	S
C19	C96	1.622	.	S
C19	C94	1.622	.	S
C19	C31	1.521	.	S

C20	C109	1.622	.	S
C20	C128	1.622	.	S
C20	C132	1.622	.	S
C20	C32	1.521	.	S
C21	C67	1.622	.	S
C21	C77	1.622	.	S
C21	C72	1.622	.	S
C21	C24	1.521	.	S
C22	C108	1.622	.	S
C22	C130	1.622	.	S
C22	C134	1.622	.	S
C22	C23	1.521	.	S
C23	C24	1.238	.	T
C25	C26	1.238	.	T
C26	C136	1.521	1_455	S
C27	C28	1.238	.	T
C28	C137	1.520	1_455	S
C29	C30	1.238	.	T
C31	C32	1.238	.	T
C33	C34	1.238	.	T
C34	C135	1.521	1_455	S
C35	C36	1.238	.	T
C37	C38	1.238	.	T
C37	C112	1.520	1_554	S
C39	C40	1.238	.	T
C39	C140	1.520	1_444	S
C41	C42	1.238	.	T
C41	C124	1.520	1_545	S
C43	C44	1.238	.	T
C43	C123	1.520	1_545	S
C45	C46	1.238	.	T
C46	C122	1.521	1_545	S
C47	C48	1.238	.	T
C48	C110	1.520	1_554	S
C49	C50	1.238	.	T
C51	C52	1.238	.	T
C51	C111	1.520	1_554	S
C53	C54	1.238	.	T
C55	C56	1.302	.	T
C57	C58	1.302	.	T
C59	C60	1.302	.	T
C61	C62	1.302	.	T
C63	C64	1.302	.	T
C65	C66	1.302	.	T
C67	C68	1.302	.	T

C69	C70	1.302	.	T
C71	C72	1.302	.	T
C73	C74	1.302	.	T
C75	C76	1.302	.	T
C77	C78	1.302	.	T
C79	C80	1.302	.	T
C81	C82	1.302	.	T
C83	C84	1.302	.	T
C85	C86	1.303	.	T
C87	C88	1.302	.	T
C89	C90	1.302	.	T
C91	C92	1.302	.	T
C93	C94	1.302	.	T
C95	C96	1.302	.	T
C97	C98	1.302	.	T
C99	C100	1.302	.	T
C101	C102	1.302	.	T
C103	C104	1.302	.	T
C105	C106	1.302	.	T
C107	C113	1.302	1_554	T
C107	C111	1.622	1_554	S
C108	C109	1.302	.	T
C110	C113	1.622	.	S
C110	C115	1.622	.	S
C110	C121	1.622	.	S
C110	C48	1.520	1_556	S
C111	C117	1.622	.	S
C111	C119	1.622	.	S
C111	C51	1.520	1_556	S
C111	C107	1.622	1_556	S
C112	C154	1.622	.	S
C112	C156	1.622	.	S
C112	C158	1.622	.	S
C112	C37	1.520	1_556	S
C113	C107	1.302	1_556	T
C114	C115	1.302	.	T
C116	C117	1.302	.	T
C118	C119	1.302	.	T
C120	C121	1.302	.	T
C122	C126	1.622	.	S
C122	C127	1.622	.	S
C122	C133	1.622	.	S
C122	C46	1.521	1_565	S
C123	C125	1.622	.	S
C123	C129	1.622	.	S

C123	C131	1.622	.	S
C123	C43	1.520	1_565	S
C124	C144	1.622	.	S
C124	C142	1.622	.	S
C124	C157	1.622	.	S
C124	C41	1.520	1_565	S
C125	C126	1.302	.	T
C127	C128	1.302	.	T
C129	C130	1.302	.	T
C131	C132	1.302	.	T
C133	C134	1.302	.	T
C135	C139	1.622	.	S
C135	C152	1.622	.	S
C135	C34	1.521	1_655	S
C135	C149	1.622	.	S
C136	C138	1.622	.	S
C136	C145	1.622	.	S
C136	C147	1.622	.	S
C136	C26	1.521	1_655	S
C137	C141	1.622	.	S
C137	C155	1.622	.	S
C137	C160	1.622	.	S
C137	C28	1.520	1_655	S
C138	C139	1.302	.	T
C140	C143	1.622	.	S
C140	C159	1.622	.	S
C140	C39	1.520	1_666	S
C140	C153	1.622	.	S
C141	C142	1.302	.	T
C143	C144	1.302	.	T
C145	C146	1.302	.	T
C147	C148	1.302	.	T
C149	C150	1.302	.	T
C151	C152	1.302	.	T
C153	C154	1.302	.	T
C155	C156	1.302	.	T
C157	C158	1.302	.	T
C159	C160	1.302	.	T